

Effective and anatomical connectivity of the dorso-central insula during the processing of action forms.

Di Cesare G.,^{a1} Zeidman P.^b, Lombardi G.^{ad}, Urgen B.A.^c, Sciutti A.^a

^a Italian Institute of Technology, Cognitive Architecture for Collaborative Technologies Unit, Genova, Italy.

^b Wellcome Centre for Human Neuroimaging, UCL, 12 Queen Square, London WC1N 3AR, United Kingdom.

^c Department of Psychology and Interdisciplinary Neuroscience Program, Bilkent University, Ankara, 06800, Turkey; Aysel Sabuncu Brain Research Center & National Magnetic Resonance Research Center (UMRAM), Bilkent University, Ankara, Turkey.

^d Department of Informatics, Bioengineering, Robotics and Systems Engineering (DIBRIS), University of Genoa, Genoa, Italy

¹Corresponding author: giuseppe.dicesare@unipr.it

Abstract

In both human and monkeys the observation and execution of actions produced the activation of a network consisting of parietal and frontal areas. Although this network is involved in the encoding of the action goal, it does not consider the affective component of the action: *vitality form* (VF). Several studies showed that the observation and execution of actions conveying VFs selectively activated the dorso-central insula (DCI). In the present study, we aimed to clarify, by using Dynamic Causal Modeling (DCM), the direction of the information flow across DCI, parieto-frontal areas (PMv, IPL) and posterior superior temporal sulcus (pSTS) during both observation and execution of actions conveying VFs. Results indicate that, during observation, DCI receives the visual input from pSTS, and, in turn, sends it to the fronto-parietal network. Moreover, DCI significantly modulates PMv. Conversely, during execution, the motor input starts from PMv, reaches DCI and IPL, with a significant modulation from PMv to DCI. The reciprocal exchange of information between PMv and DCI suggests that these areas work closely together in the VFs

action processing. An additional tractography analysis corroborates our DCM models, showing a correspondence between functional connections and anatomical tracts.

1. Introduction

Several studies have demonstrated, both in monkeys and humans, the existence of a network characterized by cortical areas activated during the observation and execution of goal-directed actions, such as grasping an object [1-6]. This network mainly includes the inferior parietal lobule (IPL) and the ventral premotor cortex (PMv). In addition, the posterior superior temporal sulcus (pSTS) was also found to be active during the observation of actions, suggesting that this area is thought to be the source of higher-order visual input for the parieto-frontal circuit [7]. It is important to note that, although this network is involved in the encoding of the *action content* (the goal), it does not take into account another fundamental aspect: the *action form* (how the goal is achieved). For example, an action such as passing a bottle, may be executed in different ways (gently, rudely). The same goes for communicative gestures, such as greeting someone with a delicate or vigorous handshake. According to Stern [8], these forms of action are named *vitality forms*. In the last few years, several fMRI studies have shown that the observation of actions endowed with vitality forms produced, in addition to the parieto-frontal network, selective activation of the dorso-central insula (DCI). Notably, also the execution of the same actions activated the same insular sector [9,10], highlighting the role of DCI during the perception and expression of actions conveying different vitality forms.

According to Kurth et al. [11], the insula can be divided in four main functional domains: the sensorimotor (in which the DCI is located), socioemotional, olfactory–gustatory, and cognitive ones. Moreover, the insula is considered a sensory “interoceptive cortex” that integrates homeostatic, visceral, nociceptive, and somatosensory inputs, through which a representation of the internal state of the body is generated [12]. These findings indicate that the insula has several afferent and efferent connections, related to different parts of the body, through which this area can

modulate different motor behaviors. It has been proposed that, during the execution of an action, DCI may transform information regarding the affective state of the agent (positive, negative) into a specific vitality form (gentle, rude) [13]. This hypothesis is supported by empirical evidence concerning the connectivity of the dorso-central insula with brain regions involved in the action observation-execution network [14] as well as with temporal areas encoding visual biological stimuli [15]. Based on these findings, an interesting issue to investigate is the role of DCI in relation to the parieto-frontal network during the observation and execution of action vitality forms. For this purpose, the present study aims to clarify the direction of the information flow across DCI, pSTS, PMv and IPL, establishing their causal role during the observation and execution of vitality forms. By using Dynamic Causal Modeling (DCM) [16,17], we analyzed data collected in a previous fMRI study [13] in which participants were required to perform two tasks: 1) observe an arm action (observation task, OBS); 2) execute the same action (execution task, EXE). In the OBS task, participants observed video clips showing the right arm of an actor performing actions towards another actor with vitality forms (gentle, rude) or without vitality forms (i.e., jerky actions; control condition). In the EXE task, participants moved an object located on a plane, as if offering it to the other person, with a gentle or rude vitality form (vitality form condition) or without vitality form (control condition). We hypothesized a modulation effect of DCI on the parieto-frontal areas in both OBS and EXE tasks.

2. Materials and methods

In the present study we analyzed fMRI data previously collected by Di Cesare and colleagues [13]. In the following text details on methods are provided.

2.1. Participants

Sixteen healthy right-handed volunteers (nine females and seven males, mean age = 25.4, SD = 2) took part in the fMRI experiment. All participants had normal or corrected-to-normal visual acuity.

None of them reported a history of psychiatric or neurological disorders or current use of any psychoactive medications. They gave their written informed consent to be subjected to the experimental procedure, which was approved by the Local Ethics Committee of Parma (552/2020/SPER/UNIPR) in accordance with the Declaration of Helsinki. All regions of interest (ROIs) essential for DCM analysis were identified in 15 subjects, so those subjects were included in the DCM analysis.

2.2. Experimental Design and Stimuli

The experiment was presented as a blocked design. It was based on a 2 x 2 factorial design with task (observation, OBS; execution, EXE) and conditions (Vitality forms; Control) as factors. In total, four conditions were presented in independent mini blocks (VF OBS, VF EXE, CT OBS, CT EXE) in a randomized order. Each mini-block presented four video-clips. Each video-clip lasted 3s. A total of 12 visual stimuli were presented during the OBS task: 8 for vitality forms condition (4 objects x 2 vitality forms) and 4 for the control condition (4 objects x 1 jerky action). A total of 3 passing actions were requested during the EXE task: 2 for vitality forms condition (1 object x 2 vitality forms) and 1 for the control condition (1 object x 1 jerky action). In OBS task, participants were presented with video-clips showing the right hand of an actor performing four leftward passing actions towards another actor sitting in front of the first one, using two different vitality forms (gentle and rude; Figure 1). The actions observed consisted in passing four different objects (a packet of crackers, a ball, a cup, a bottle). Additionally, video-clips also showed the same actions performed in a jerky way (Control condition; Figure 1). Specifically, control stimuli were obtained by presenting one static frame of the action every 700ms (4 frames in total from the beginning to the end of the action). The aim of the control stimuli was to allow participants to understand the action goal without conveying any vitality form information. During the EXE task, we presented a static image of the actor seated opposite the observer and asked participants to move a little box towards the actor with vitality forms (gentle or rude) or without vitality forms by simply rotating the wrist (Figure 1). A cue positioned in the center of the screen indicated when to start the action,

and the color of the screen edge indicated the vitality form through which the action had to be executed (blue color: gentle; red color: rude; gray color: neutral, Figure 1). In each video, a fixation cross was introduced to control for restrained eye movements. To avoid possible repetition suppression effect in the vitality form condition, we changed randomly the vitality forms of both observed and performed actions.

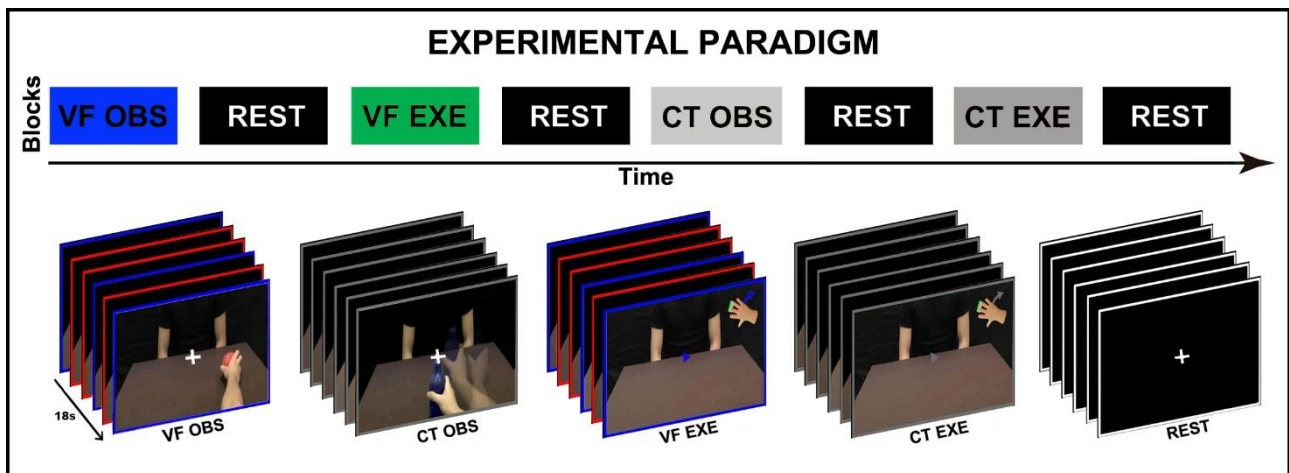


Figure 1. Experimental Paradigm. In the observation task, participants were asked either to pay attention to the action vitality form (vitality form condition, VF OBS) or to observe the jerky action (control condition, CT OBS). In the execution task, participants were asked to perform the action gently (blue color, rudely (red color, vitality form condition, EXE VF) or neutrally (control condition, CT EXE). Before the presentation of stimuli, an initial text panel instructed participants about the task to perform. Between blocks an inter-block interval lasting 18s was presented (Rest).

2.3. Paradigm

During the experiment, participants laid in the scanner in a dimly lit environment. The stimuli were presented via digital visors (VisuaSTIM) with a 500,000 px x 0.25 square inch resolution and horizontal eye field of 30°. The digital transmission of the signal to the scanner was via optic fiber. The software E-Prime 2 Professional (Psychology Software Tools, Inc., Pittsburgh, USA, <http://www.pstnet.com>) was used for stimuli presentation. The experiment consisted into 2 runs. Each functional run lasted about 10min. In each run, the experimental stimuli were presented in blocks consisting of four consecutive stimuli (each lasting 3s) of the same condition (VF OBS, CT OBS, VF EXE, CT EXE; Figure 1). Each run consisted in 4 blocks for each condition, presented in a randomized order. Between experimental blocks, inter-blocks in which participants were asked only to observe a white cross (rest period) were presented. During the OBS task participants

observed 36 actions for each condition (VF OBS, CT OBS), while for the EXE task they performed 36 actions for each condition (VF EXE, CT EXE).

2.4. Image acquisition, preprocessing and first-level analysis

Anatomical T1-weighted and functional T2*-weighted MR images were acquired with a 3 Tesla General Electrics scanner equipped with an 8-channel receiver head-coil. Functional images were acquired using a T2*-weighted gradient-echo, echo-planar (EPI) pulse sequence acceleration factor 2, 40 sequential transverse slices (slice thickness = 3 plus inter-slice gap = 0.5 mm) covering the whole brain, with a TR time of 3000ms (TE = 30ms, flip-angle = 90 degrees, FOV = 205 x 205 mm², in-plane resolution 2.5 x 2.5 mm²). The experiment consisted of two functional runs. Each functional run comprised 169 ascending interleaved volumes. Additionally, a T1 weighted structural image was acquired for each participant (acceleration factor 2, 156 sagittal slices, matrix 256x256, isotropic resolution 1x1x1 mm³, TI=450ms, TR =8100ms, TE = 3.2ms, flip angle 12°). For each subject, fMRI data were pre-processed with standard procedures including motion correction, slice-time correction (referenced to 1st slice in the series), normalization, and smoothing (6 mm) using the SPM12 software. For all subjects, head motion was carefully checked along x (pitch movement), y (yaw movement) and z (roll movement) directions and no participant has met the exclusion criteria of 3mm mean displacement (translation > 3mm or rotation > 3°). Data were analyzed using a random-effects model, implemented in a two-level procedure. In the first level, single-subject fMRI BOLD signal was modelled in a General Linear Model (GLM) by a design-matrix comprising the onsets, the durations of each event according to the experimental task for each functional run. In the experiment, at first level GLM comprised the following regressors: Vitality Observation (VF OBS), Control Observation (CT OBS), Vitality Execution (VF EXE), Control Execution (CT EXE) and Instruction. Within each block, the videos were modelled as a whole event lasting 18s. The instruction was modelled with a duration of 3s. In the second level analysis (group-analysis), corresponding contrast images of the first level for each participant were entered into a flexible ANOVA with sphericity-correction for repeated measures. This model was

composed of 4 regressors (VF OBS, CT OBS, VF EXE, CT EXE) and considered the activation pattern obtained for different tasks (OBS, EXE) in two different conditions (vitality and control). Within this model, we assessed activations associated with each task versus implicit baseline and activations resulting from the direct contrast between conditions (VF OBS vs. CT OBS, VF EXE vs. CT EXE; PFWE <0.05 corrected at the cluster level). To identify the overall activity patterns involved in both the observation and execution of vitality forms, a conjunction analysis was carried out (OBS VF & EXE VF). After the identification of the activity pattern four core nodes were identified: posterior superior temporal sulcus (pSTS), inferior parietal lobe (IPL), ventral premotor cortex (PMv) and dorso-central insula (DCI) (Figure 2). Then, for each participant, by using the first-level analysis, four ROIs were created (pSTS, IPL, PMv and DCI) around the local maxima obtained from both the contrasts *VF OBS vs. baseline* and *VF EXE vs. baseline* ($p < 0.001$ uncorrected). Finally, for each ROI, the time series data was extracted by using the principal eigenvariate of all voxels (that survived the threshold of $p < 0.05$) within a sphere of 5mm radius.

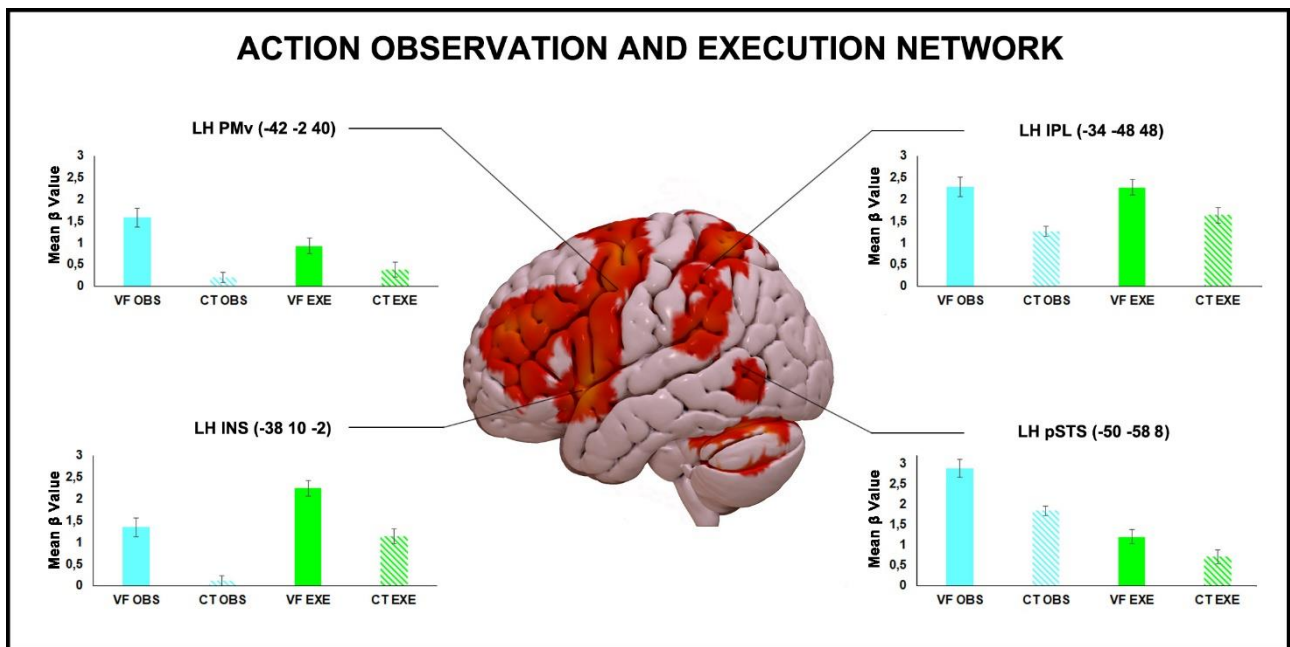


Figure 2. Brain activations resulting from the conjunction analysis between the contrasts *VF observation vs. baseline* and *VF execution vs. baseline*. These activations are rendered into a standard MNI brain template (pFWE<0.05 at voxel level).

2.5. Specification of the network models

The aim of the present study was to identify the best model that clarifies the direction of vitality from information flow during the observation and execution of actions performed rudely or gently. For this purpose, we focused on four main nodes involved in actions observation and execution: pSTS, IPL, PMv and DCI. Information on the anatomical connectivity of these regions come from monkeys and humans investigations.

IPL-PMv-pSTS connectivity

Previous studies showed that, in the macaque monkeys, the inferior parietal lobule (IPL) is a brain area involved in the planning and the execution of motor tasks. In particular, single neuron studies demonstrated that areas PG and PFG of IPL are activated during arm and hand movements respectively [3]. Additionally, the parietal area PFG is strongly connected to the ventral premotor areas, especially area F5 [18] and to the posterior part of the superior temporal sulcus (pSTS). In humans, several studies demonstrated that this circuit consists of homologous brain areas: IPL and PMv. Furthermore, as aforementioned for monkeys, also in humans STS was found to be active during the observation of actions [19].

DCI connectivity

Previous monkey studies showed that the central sector of the insula is connected to the two main nodes of the classical parieto-frontal circuit: the rostral IPL area and the premotor area F5 [6,20]. Moreover, DCI appears to correspond to the portion of the macaque insula connected with the grasping circuit [21] and where electrical microstimulation evokes hand movements [22]. Furthermore, Augustine showed anatomical connections of this insular sector with the temporal pole and the superior temporal sulcus of the temporal lobe in monkeys [23]. These data are in line with Ghaziri and colleagues who demonstrated, in humans, a functional connectivity between DCI and STS [24]. Moreover, a probabilistic tractography study carried out on both humans and

monkeys, showed that DCI is anatomically connected with the parieto-frontal circuits involved in the reaching/grasping network [14].

Based on these anatomical findings, pSTS, IPL, PMv and DCI are suitable nodes to investigate the direction of vitality form information flow, by establishing their causal role during action observation and execution respectively. To this aim, fMRI data were analyzed with dynamical causal modeling (DCM), a technique able to estimate the effective connectivity between different regions of interest [25]. Particularly, DCM consists of two steps: 1) model specification-estimation; 2) model selection. In the first step, several possible models are specified based on known anatomical connections between regions of interest and hypothetical modulation of these regions. In the second step, Bayesian Model Selection (BMS) procedure is used to determine the most likely model that generated the observed data. During this procedure, a probability value is assigned to each model for the explanation of the observed data. The model with the highest probability is considered the *winning* model. In our study, 8 models were hypothesized for each task (OBS, EXE). All these models considered the four ROIs that are activated in the left hemisphere during both the observation and execution of vitality forms: pSTS, IPL, PMv, DCI (coordinates are listed in Table 1). Based on the anatomical-functional constraints described above, we considered the intrinsic connectivity including forward and backward connections between all these regions (Figures 3).

DCM Nodes	OBS Task				EXE Task			
	x	y	z	SEM	x	y	z	SEM
pSTS	-50	-58	6	0.3 1.2 0.5	-49	-57	5	0.4 1.1 0.8
IPL	-33	-47	48	0.4 0.6 0.9	-33	-46	48	0.4 0.8 1.0
PMv	-42	-2	41	0.4 0.5 1.0	-42	-2	41	0.4 0.6 1.0
DCI	-38	10	2	0.5 1.5 1.1	-38	10	0	0.3 0.8 0.6

Table 1. MNI coordinates of central voxels of the ROIs used in DCM analysis averaged across subjects.

For the OBS and EXE tasks, we defined 8 models considering all the possible patterns of modulatory effect. Moreover, for each model, pSTS, and PMv were hypothesized to be the nodes where the visual input and motor input could enter in the system and then reach the other areas of the network (Figure 3).

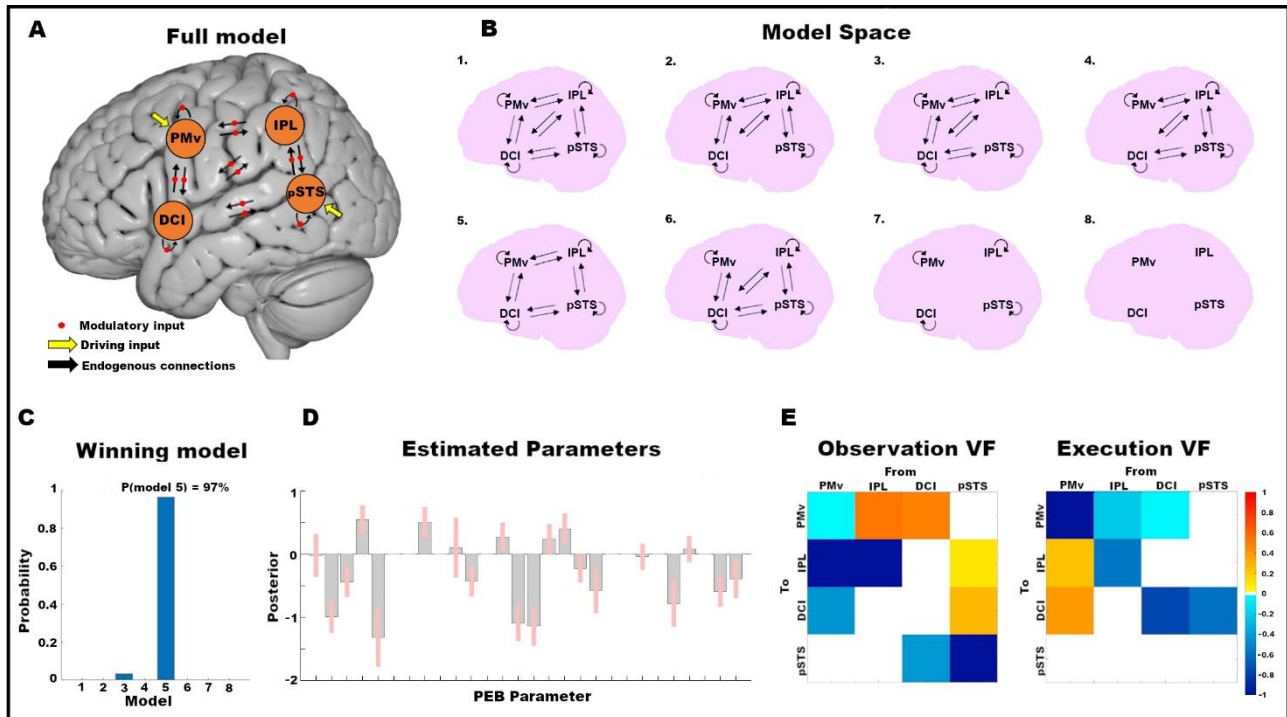


Figure 3. The “full” DCM structure (A). Black arrows represent endogenous connections (A matrix). Yellow arrows represent driving inputs entering in PMv (EXE) and pSTS (OBS). Red dots represent modulatory inputs VF EXE and VF OBS (B matrix) which were enabled to modulate all connections, including self-inhibitory ones (curved black arrows). Model space including the “full” model (1), six reduced models (2-7) in which we switched off the modulatory inputs entering in specific connections and a “null” model (8) with no modulation serving as baseline (B). The best model was number 5 (connections between DCI and IPL are not modulated) with a posterior probability of 97% (C). Bayesian Model Average (BMA) of the parameters which survived a thresholding at posterior probability >95% (D). Effective connectivity matrices (E). For off-diagonal values, connection strengths (Hz) are represented in a scale from yellow to red, if excitatory, and from turquoise to blue, if inhibitory. For leading diagonal values, representative of self-connectivity, which is inhibitory for definition, the colour code is inverted (negative mean disinhibition).

In the specification of DCM models, default parameters in SPM12 were used: Modulatory effects were specified to be bilinear, one-state model was run for each region, and stochastic effects were not modeled. Once the parameters were estimated for each model at the individual subject level, random-effects analysis Bayesian Model Average (BMA) was used to determine the *winning* model at the group level. This method determines a probability for each model, known as the exceedance probability, by pooling the evidence from all subjects. This probability indicates that a model is more likely than any other tested model. Once the *winning* model was determined, each of the

intrinsic connection strengths and *modulatory connection effects* were analyzed to identify the significant connections. The *intrinsic connection strengths* indicate the strength of the connectivity between two ROIs. On the other hand, the *modulatory connection effects* indicate the change in the effective connectivity value of a connection due to an experimental manipulation. All connections are measured in Hz. Note that positive values indicate strong connections while negative values indicate weak connections.

3. Results

Results of the PEB analysis showed that model 5 is the one which best explained our data, with a poster probability of 97% (Figure 3C). This model excludes the connections between DCI and IPL from the modulation effect of vitality forms during both the observation and execution tasks. By thresholding the BMA at >95% posterior probability (thresholding based on the free energy), we found parameters characterized by strong evidence of being present versus absent (Figure 3D). These parameters are also shown in Figure 3E in form of connectivity matrices in which a positive sign (yellow and orange squares) represents excitatory influences while a negative sign (turquoise and blue squares) represents inhibitory influences except for self-connections (diagonal), which are inhibitory by definition. Thus, positive self-connections represent more inhibition and negative self-connections represent disinhibition. Considering between-regions connectivity, during the observation of vitality forms results revealed a positive modulation of the connections from DCI to PMv (0.5), from IPL to PMv (0.53), from pSTS to IPL (0.12) and from pSTS to DCI (0.3) (Figure 4A1). During the execution of vitality forms, results revealed a positive modulation of the connections from PMv to IPL (0.24) and from PMv to DCI (0.42) (Figure 4B1). Additionally, results showed a strong disinhibition effect of IPL (-1.32) and pSTS (-1.08) during the observation of vitality forms (Figure 3E left panel) and of PMv (-1.14), IPL (-0.57) and DCI (-0.78) during the execution of vitality forms (Figure 3E right panel). The data-driven automatic search over parameters identified a network with very similar connection strengths. Particularly, the automatic search showed a positive modulation (thresholding at 95% posterior probability) of the connections

from IPL to PMv (0.56), from DCI to PMv (0.48) and a disinhibition effect of IPL (-1.40) and pSTS (-0.99) during the observation of vitality forms.

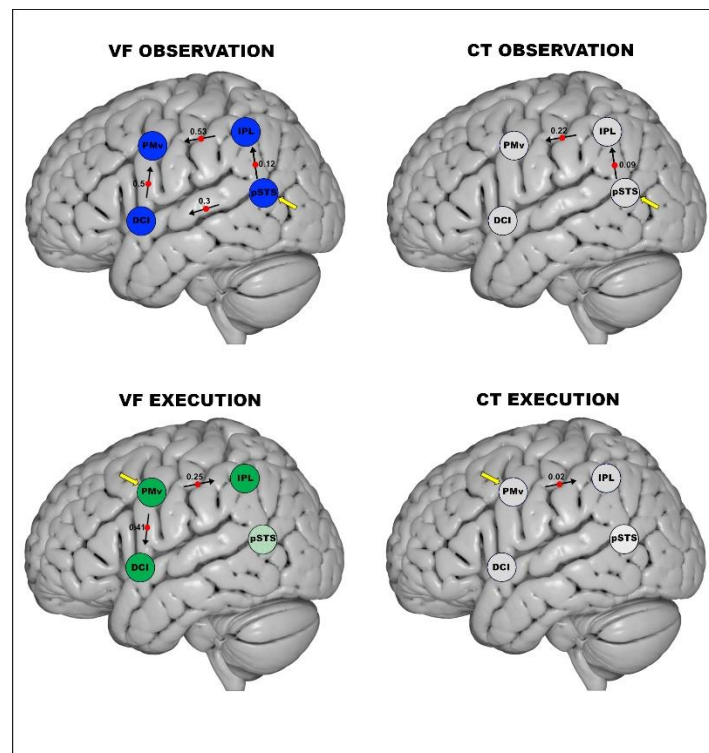


Figure 4. Modulatory connection strengths in the winning models relative to the OBS and EXE tasks surviving at BMA thresholding at 95% posterior probability (strong evidence). Red dots represent positive modulation effects during the VFs observation (A1), control observation (A2), VFs execution (B1) and control execution (B2). Yellow arrows indicate driving inputs where the visual and motor information of action starts.

In addition, it found a positive modulation (thresholding at 95% posterior probability) of the connections from PMv to DCI (0.36) and a disinhibition effect of PMv (-1.05), IPL (-0.69) and DCI (-0.82) during the execution of vitality forms. Finally, to verify the specificity of the winning model 5 for vitality forms observation and execution, we tested how the communication between its nodes were modulated by the control conditions, consisting in the observation (CT OBS) and execution (CT EXE) of neutral actions with constant velocity. Results after BMA thresholding (95% posterior probability) revealed a positive modulation of CT OBS on the connections from pSTS to IPL (0.09) and from IPL to PMv (0.22) (Figure 4A2) and a positive modulation of CT EXE on the connection from PMv to IPL (0.02) (Figure 4B2). Notably, connectivity parameters including DCI did not survive to the BMA thresholding, suggesting the involving of DCI only during vitality forms processing.

Results of Diffusion Analysis

In order to identify anatomical tracts corresponding to the effective connections of the two winning models, an additional tractography analysis (DTI) was carried out on the same group of participants. Specifically, diffusion data collected by Di Cesare et al. [13], already pre-processed with the FMRIB Software Library (FSL) tools (version 5.0.9), were analyzed with FSL's PROBTRACKX tool. The seed points used for the probabilistic tractography analysis corresponded to ROI's identified in the DCM analysis (PMv, x -42 y -2 z 40; IPL, x -34 y -48 z 46; INS x -38 y 10 z -2; pSTS, x -50 y -58 z 8; Figure 2). Figure 5 shows anatomical tracts connecting ROIs: pSTS-DCI, DCI-PMv, DCI-IPL, PMv-IPL. These anatomical findings corroborate DCM data described above, indicating the existence of a network able to process vitality forms during both OBS and EXE tasks.

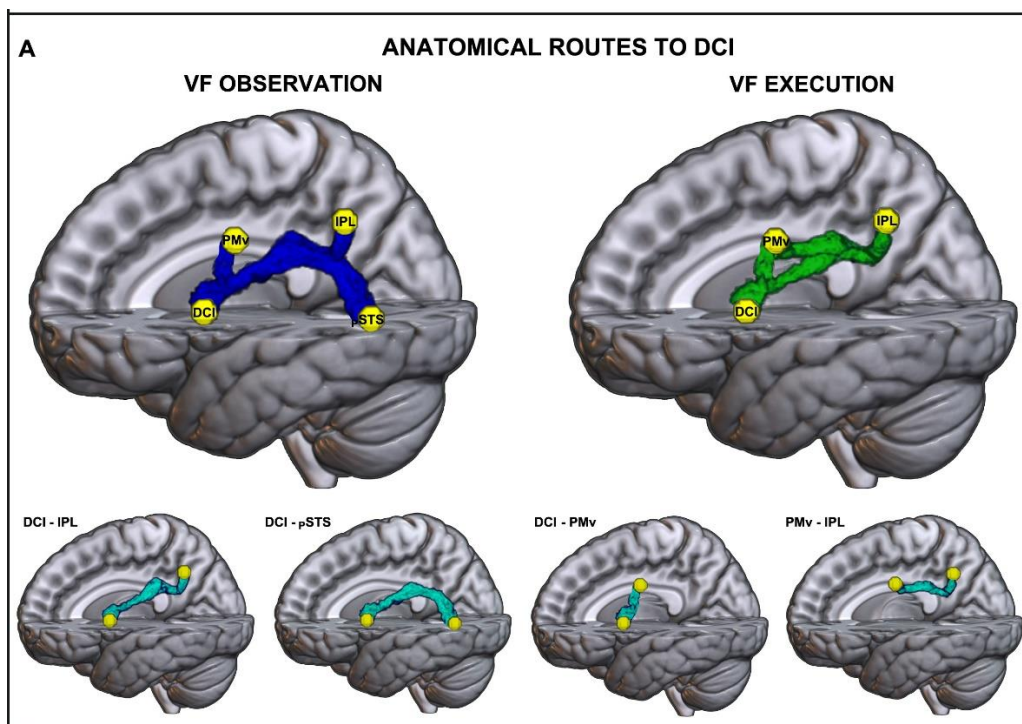


Figure 5. Results of tractography analysis showing the white-matter tracts corresponding to the effective connections of the winning model identified for the OBS and EXE tasks.

4. Discussion

In both humans and monkeys, the observation and execution of actions produced the activation of parietal and frontal areas involved in the action goal processing. In particular, several studies have shown that, in macaque monkeys, this network mainly includes area F5 of the premotor cortex and

several areas of IPL [2,3,6]. A similar network was also found in humans, involving the inferior parietal lobule (IPL) and the ventral premotor cortex (PMv) [1,4,5,7].

Besides the goal, another fundamental aspect of the action concerns the way in which it is performed (i.e. action form). Indeed, when we interact with others, the same action may be performed in different ways. For example, when we meet a person, we can greet him/her vigorously or weakly, reflecting if we are really happy to see him/her or if our gesture is a merely greeting of circumstance. Conversely, the observation of actions conveying different vitality forms allows us to understand the positive or negative attitude of the agent. In the last years, several fMRI studies provided evidence that, besides the activation of the parieto-frontal network, the observation and the execution of actions expressed gently and rudely produced a selective activation of the dorso-central insula (DCI) and of the middle cingulate cortex (MCC) [13]. These findings suggest that, while the parieto-frontal network is involved in the *action goal* processing, the DCI-MCC circuit is involved in the *action form* processing. An interesting issue to clarify is whether and how these two circuits functionally interact during the encoding of actions. Recent anatomical findings showed that, in both humans and monkeys, the dorso-central insula is connected to the parieto-frontal network, thus highlighting the role of DCI as the crossroads between these two circuits during the processing of vitality forms. In this view, we hypothesized that, during the observation of an action, DCI may receive information from pSTS, and encode physical features of the action, allowing the observer to infer the affective state of the agent. Conversely, during the execution of an action, DCI may transform information regarding the affective state of the agent (i.e positive, negative) into a specific vitality form, modulating the execution of actions via parieto-frontal network. In order to address this issue, the present study aimed to investigate, by using Dynamic Causal Modeling (DCM), the direction of the information flow across DCI, pSTS, PMv and IPL, establishing their causal role in the observation and execution of vitality forms. Specifically, we analyzed fMRI data regarding two tasks: 1) observation task, in which participants observed video-clips showing passing actions performed with vitality forms (gentle, rude) or without vitality forms (i.e., jerky

actions; control condition); 2) execution task, in which participants performed the same actions with or without vitality forms.

The Results showed that, during action observation, visual information reaches pSTS. From here two visual streams depart, one towards IPL, concerning action goal and one towards DCI, concerning action vitality forms. During action execution, motor information starts from PMv. From this node two streams depart, one, concerning the action goal, towards IPL and one, concerning the action vitality form, towards DCI. This last finding was unexpected because indicates that PMv could contain a vocabulary of actions tagged with specific vitality forms.

On the basis of our DCM model, it is plausible that, during action observation, the DCI transforms the affective component characterizing vitality forms into physical features and sends this information to PMv. The role of DCI in this transformation has been already addressed in a previous fMRI study conducted by Di Cesare and colleagues [28]. Specifically, in this study participants were presented with several videos showing hand-arm actions and were asked to judge either their vitality form (gentle, neutral, rude) or their velocity (slow, medium, fast). Results of a multi-voxel pattern analysis showed that, in the DCI, there were voxels selectively tuned to vitality forms, while voxels selectively tuned to velocity were rare. These findings suggest that vitality forms are encoded by specific features related to the affective component of actions, which are not simply related to the velocity.

Regarding the EXE task, that the motor information starts from PMv, reaches DCI and IPL, Notably, we found a significant modulation from PMv to DCI during the action execution. It is well known that, both in monkeys and humans, the premotor cortex and parietal areas are activated during the execution of actions. Concerning the functional role of these brain areas, Chersi and colleagues [29] proposed that, during the execution of an action, IPL is involved in the planning of different motor acts constituting that action. For example, during a placing movement, several neural populations become sequentially active, encoding different parts of the action such as reaching the object, shaping the hand, grasping the object and then placing it (intentional action

chains). Then, this planning information is transmitted to the premotor cortex. Several studies showed that the premotor cortex of monkeys contains neurons encoding different types of action, such as grasping, holding, tearing, etc., encoded by different neuron populations, forming an “action storage” (vocabulary of motor acts) [30]. On the basis of the planned action, specific motor acts are selected from the premotor cortex vocabulary. Finally, this information is transmitted to the primary motor cortex (M1) which, in turn, starts the movement. Notably, our DCM model takes also in consideration the involvement of DCI during the execution of actions. Specifically, DCM model shows a significant modulation effect PMv towards DCI indicating that, according to the positive/negative attitude of the agent, PMv selects the right motor program to execute (gentle or rude action) and send this information to DCI which may add the affective component to these actions, allowing the agent to feel rude or gentle during the action execution.

Results of effective connectivity among DCI, pSTS, PMv and IPL is corroborated by an additional tractography analysis (DTI) carried out on the same group of participants. Specifically, each intrinsic connection resulting from DCM analysis relies on an anatomical tract found in DTI analysis. Taken together, results of DCM and DTI analyses show a correspondence between functional connections and anatomical routes.

References

1. Rizzolatti G., & Sinigaglia C. (2016). The mirror mechanism: A basic principle of brain function. *Nature Reviews Neuroscience*, 17(12), 757- 765. <https://doi.org/10.1038/nrn.2016.135>
2. Rizzolatti G., Fadiga L., Gallese V., Fogassi L. (1996). Premotor cortex and the recognition of motor actions. *Brain Res. Cogn. Brain Res.* **3**, 131–141. (10.1016/0926-6410(95)00038-0)
3. Rozzi S., Ferrari P.F., Bonini L., Rizzolatti G., Fogassi L. (2008). Functional organization of inferior parietal lobule convexity in the macaque monkey: electrophysiological characterization of motor, sensory and mirror responses and their correlation with cytoarchitectonic areas. *Eur. J. Neurosci.* 28, 1569–1588. (10.1111/j.1460-9568.2008.06395.x)

4. Rizzolatti G., & Luppino G. (2001). The cortical motor system. *Neuron*, 31(6), 889–901. [https://doi.org/10.1016/s0896-6273\(01\)00423-8](https://doi.org/10.1016/s0896-6273(01)00423-8)
5. Rizzolatti G., & Craighero L. (2004). The mirror-neuron system. *Annual review of neuroscience*, 27, 169–192. <https://doi.org/10.1146/annurev.neuro.27.070203.144230>
6. Bruni S., Gerbella M., Bonini L. et al. (2018) Cortical and subcortical connections of parietal and premotor nodes of the monkey hand mirror neuron network. *Brain Struct Funct* 223, 1713–1729. <https://doi.org/10.1007/s00429-017-1582-0>
7. Rizzolatti G., Fogassi L., (2014) The mirror mechanism: recent findings and perspectives. *Philos Trans R Soc Lond B Biol Sci*, Apr 28;369(1644):20130420. doi: 10.1098/rstb.2013.0420.
8. Stern D.N., (1985) *The Interpersonal World of the Infant*, New York Basic Book
9. Di Cesare G., Di Dio C., Marchi M., Rizzolatti G., (2015) Expressing our internal states and understanding those of others. *PNAS USA*, Aug 4; 112 (33) 10331-10335. <https://doi.org/10.1073/pnas.1512133112>
10. Di Cesare G., Gerbella M., Rizzolatti G. The neural bases of vitality forms. *Natl Sci Rev*. 2020 Jan;7(1):202-213. doi: 10.1093/nsr/nwz187. Epub 2020 Feb 24. PMID: 34692032; PMCID: PMC8288905.
11. Kurth F., Zilles K., Fox PT., Laird AR., Eickhoff SB. (2010) A link between the systems: functional differentiation and integration within the human insula revealed by meta-analysis. *Brain Struct Funct*, June; 214: 519-534. doi:10.1007/s00429-010-0255-z
12. Craig AD (2002) How do you feel? Interoception: the sense of the physiological condition of the body. *Nat Rev Neurosci*, Aug; 3:655–666. doi: 10.1038/nrn894
13. Di Cesare G., Marchi M., Lombardi G., Gerbella M., Sciutti A., Rizzolatti G. (2021). The middle cingulate cortex and dorso-central insula: A mirror circuit encoding observation and execution of vitality forms. *PNAS USA*, Nov 2;118(44):e2111358118. doi: 10.1073/pnas.2111358118.

14. Di Cesare G., Pinardi C., Carapelli C., Caruana F., Marchi M., Gerbella M., Rizzolatti G., (2019) Insula Connections With the Parieto-Frontal Circuit for Generating Arm Actions in Humans and Macaque Monkeys. *Cerebral Cortex*, May; 29 (5) 2140–2147. <https://doi.org/10.1093/cercor/bhy095>
15. Almashaikhi T., Rheims S., Jung J., Ostrowsky-Coste K., Montavont A., De Bellescize J., Arzimanoglou A., Kosal PK., Guénot M., Bertrand O., Ryvlin P. (2014) Functional connectivity of insular efferences. *Human Brain Mapping*, May; 35(10) 5279-5294. <https://doi.org/10.1002/hbm.22549>
16. Friston K.J., Harrison L., & Penny W. (2003). Dynamic causal modelling. *Neuroimage*, 19(4), 1273-1302.
17. Penny W.D., Stephan K.E., Mechelli A., & Friston K.J. (2004). Modelling functional integration: a comparison of structural equation and dynamic causal models. *Neuroimage*, 23, S264-S274
18. Rozzi S., Calzavara R., Belmalih A., Borra E., Gregoriou G.G., Matelli M., & Luppino G., (2006) Cortical Connections of the inferior parietal cortical convexity of the macaque monkey. *Cereb Cortex*, 16, 1389-1417, doi:10.1093/cercor/bhj076
19. Filimon F., Nelson J. D., Hagler D. J., & Sereno M. I. (2007). Human cortical representations for reaching: mirror neurons for execution, observation, and imagery. *NeuroImage*, 37(4), 1315–1328. <https://doi.org/10.1016/j.neuroimage.2007.06.008>
20. Gerbella M., Borra E., Tonelli S., Rozzi S. & Luppino G. (2013) Connectional heterogeneity of the ventral part of the macaque area 46. *Cereb Cortex*, 23, 967-987. <https://doi.org/10.1093/cercor/bhs096>
21. Jezzini A., Rozzi S., Borra E., Gallese V., Caruana F. & Gerbella M. (2015). A shared neural network for emotional expression and perception: an anatomical study in the macaque monkey. *Front Behav Neurosci*, 9, 1-17. <https://doi.org/10.3389/fnbeh.2015.00243>

22. Jezzini A., Caruana F., Stoianov I., Gallese V., & Rizzolatti G. (2012). Functional organization of the insula and inner perisylvian regions. *Proceedings of the national academy of sciences*, *109*(25), 10077-10082.
23. Augustine J.R. (1996). Circuitry and functional aspects of the insular lobe in primates including humans. *Brain research. Brain research reviews*, *22*(3), 229–244. [https://doi.org/10.1016/s0165-0173\(96\)00011-2](https://doi.org/10.1016/s0165-0173(96)00011-2)
24. Ghaziri J., Tucholka A., Girard G., Houde J. C., Boucher O., Gilbert G., Descoteaux M., Lippé S., Rainville P., & Nguyen D.K. (2017). The Corticocortical Structural Connectivity of the Human Insula. *Cerebral cortex (New York, N.Y.: 1991)*, *27*(2), 1216–1228. <https://doi.org/10.1093/cercor/bhv308>
25. Friston K.J., Harrison L., & Penny W. (2003). Dynamic causal modelling. *NeuroImage*, *19*(4), 1273–1302. [https://doi.org/10.1016/s1053-8119\(03\)00202-7](https://doi.org/10.1016/s1053-8119(03)00202-7)
26. Di Dio C., Di Cesare G., Higuchi S., Roberts N., Vogt S., & Rizzolatti G. (2013). The neural correlates of velocity processing during the observation of a biological effector in the parietal and premotor cortex. *Neuroimage*, *64*, 425-436
27. Casile A., Dayan E., Caggiano V., Hendler T., Flash T., Giese M.A., Neuronal Encoding of Human Kinematic Invariants during Action Observation, *Cerebral Cortex*, Volume 20, Issue 7, July 2010, Pages 1647–1655, <https://doi.org/10.1093/cercor/bhp229>
28. Di Cesare G., Valente G., Di Dio, C., Ruffaldi E., Bergamasco M., Goebel R., & Rizzolatti G. (2016). Vitality forms processing in the insula during action observation: a multivoxel pattern analysis. *Frontiers in human neuroscience*, *10*, 267 <https://doi.org/10.3389/fnhum.2016.00267>
29. Chersi F. (2011). Neural mechanisms and models underlying joint action. *Experimental brain research*, *211*(3), 643-653.
30. Rizzolatti G., & Gentilucci M. (1988). Motor and visual-motor functions of the premotor cortex. *Neurobiology of neocortex*, *42*, 269-84.